Published in final edited form as:

*Nature*. 2018 January 11; 553(7687): 208–211. doi:10.1038/nature25172.

# Precision editing of the gut microbiota ameliorates colitis

**Wenhan Zhu**[1,*], **Maria G. Winter**[1,*], **Mariana X. Byndloss**[2], **Luisella Spiga**[1], **Breck A. Duerkop**[3], **Elizabeth R. Hughes**[1], **Lisa Büttner**[1], **Everton de Lima Romão**[2], **Cassie L. Behrendt**[3], **Christopher A. Lopez**[2], **Luis Sifuentes-Dominguez**[4], **Kayci Huff-Hardy**[5], **R. Paul Wilson**[6,7], **Caroline C. Gillis**[1], **Çagla Tükel**[6], **Andrew Y. Koh**[1,4], **Ezra Burstein**[5], **Lora V. Hooper**[3,8], **Andreas J. Bäumler**[2,#], and **Sebastian E. Winter**[1,#]

[1]Department of Microbiology, University of Texas Southwestern Medical Center, 5323 Harry Hines Blvd., Dallas, TX

[2]Department of Medical Microbiology and Immunology, School of Medicine, University of California, Davis, One Shields Ave., Davis, CA

[3]Department of Immunology, University of Texas Southwestern Medical Center, 5323 Harry Hines Blvd., Dallas, TX

[4]Department of Pediatrics, University of Texas Southwestern Medical Center, 5323 Harry Hines Blvd., Dallas, TX

[5]Department of Internal Medicine, Division of Digestive & Liver Diseases, University of Texas Southwestern Medical Center, 5323 Harry Hines Blvd., Dallas, TX

[6]Department of Microbiology and Immunology, Lewis Katz School of Medicine, Temple University, 1801 N Broad St, Philadelphia, PA 19122

[8]Howard Hughes Medical Institute, University of Texas Southwestern Medical Center, 5323 Harry Hines Blvd., Dallas, TX

## Summary

Inflammatory diseases of the gastrointestinal tract are frequently associated with changes in gut microbial communities that include an expansion of facultative anaerobic bacteria of the Enterobacteriaceae family (phylum Proteobacteria), a common signature of dysbiosis ([1–8]). Here we show that a dysbiotic expansion of Enterobacteriaceae during gut inflammation could be



[#]Correspondence and requests for materials should be addressed to A.J.B. (ajbaumler@ucdavis.edu) or S.E.W. (Sebastian.Winter@UTSouthwestern.edu).

[7]Current address: GlaxoSmithKline, 1250 S. Collegeville Road Collegeville, PA 19426

[*]Authors contributed equally

Supplementary Information is linked to the online version of the paper at www.nature.com/nature.

**Author contributions.** W.Z., M.G.W., L.S., L.B., E.R., R.P.W., E.R.H, C.A.L. and C.C.G. performed and analyzed nitrate reductase activity, *in vitro* bacterial competitive growth, NF-κB induction, DSS cytotoxity experiments as well as experiments involving conventionally raised C57BL/6 mice. M.G.W., L.S., and E.R.H., performed *Il10*$^{-/-}$ mouse experiments. W.Z., M.G.W. performed inflammation analysis. C.L.B., M.G.W., L.S., and W.Z. performed germ-free mouse experiments. B.A.D. and W.Z. analyzed 16S and metagenomic data. M.X.B. analyzed the histopathology. L.S-D. and K. H-H contributed to humanized mouse experiments. L.S. and S.E.W. performed metabolite quantification. W.Z., C.T., A.Y.K., E.B., L.V.H, A.J.B., and S.E.W. designed the experiments, interpreted the data, and wrote the manuscript with contributions from all authors.

The authors declare competing financial interests: details are available in the online version of the paper.

prevented by tungstate treatment, which selectively inhibited molybdenum cofactor-dependent microbial respiratory pathways that are only operational during episodes of inflammation. In contrast, tungstate treatment caused no overt changes in the microbiota composition under homeostatic conditions. Importantly, tungstate-mediated microbiota editing reduced the severity of intestinal inflammation in murine models of colitis. We conclude that precision editing of the microbiota composition by tungstate treatment ameliorates the adverse effects of dysbiosis in the setting of gut inflammation.

In genetically susceptible rodents, a dysbiotic microbiota is vertically transmissible with the affected offspring being more likely to develop intestinal inflammation[3,9,10], suggesting that microbiota components can instigate host responses in a disease-prone setting. The close association between mucosal inflammation and gut microbiota dysbiosis poses a challenge in establishing causality between these two events. Using metagenomic sequencing, we have recently identified molybdenum cofactor (MoCo)-dependent metabolic pathways as a signature of inflammation-associated dysbiosis[11]. MoCo-dependent anaerobic respiratory enzymes and formate dehydrogenases independently contribute to the bloom of model Enterobacteriaceae such as *E. coli*[11,12]. We reasoned that identification of MoCo-dependent processes as drivers of dysbiosis would allow us to devise a strategy to manipulate microbiota metabolism and composition during gut inflammation. Selective editing of the microbiota would allow for the investigation of potential consequences of dysbiosis such as exacerbation of mucosal inflammation.

Tungsten (W) can replace molybdenum in the molybdopterin cofactor, rendering this cofactor inactive in Enterobacteriaceae[13]. Supplementation of growth media with sodium tungstate does not broadly affect growth of Enterobacteriaceae under aerobic standard laboratory conditions but abolishes anaerobic nitrate reductase activity in commensal *E. coli*, *Proteus* strains, and *Enterobacter cloacae*. ([13], Fig. 1a–c; Extended Data Fig. 1a). To test whether tungstate supplementation could negate the fitness advantage conferred by anaerobic respiration and formate oxidation *in vitro*, we analyzed anaerobic growth of wild-type *E. coli* strains (K-12 and Nissle 1917) and isogenic MoCo biosynthesis-deficient mutants (Δ*moaA*) in mucin broth supplemented with sodium tungstate (Fig. 1d–e, Extended Data Fig. 1b). In the presence of electron acceptors, such as nitrate, or formate as electron donor, the wild-type strains were recovered in higher numbers than the isogenic *moaA* mutants, while this fitness advantage was abrogated by the addition of tungstate (Fig. 1d–e, Extended Data Fig. 1b).

To investigate whether tungstate could inhibit MoCo-dependent processes in the mammalian gut, we employed a mouse model of chemically induced colitis (dextran sulfate sodium [DSS]-induced colitis) in conjunction with experimentally introduced *E. coli* indicator strains. Groups of DSS- and mock-treated C57BL/6 mice were orally inoculated with an equal mixture of the *E. coli* K-12 wild-type strain and the Δ*moaA* mutant after the onset of inflammation. Colonization of the cecum and colon lumen was assessed five days after inoculation (Fig. 1f–g, Extended Data Fig. 2a). Prior to inoculation with *E. coli* K-12, no endogenous Enterobacteriaceae family members could be isolated from these animals (data not shown). Consistent with previous results[12], the K-12 wild-type strain outcompeted the

Δ*moaA* mutant in the cecal and colonic content of DSS-treated mice (Fig. 1f). Administration of tungstate in the DSS colitis model abrogated the fitness advantage conferred by MoCo-dependent enzymes (Fig. 1f) and decreased overall numbers of *E. coli* K-12 in the gut lumen by several orders of magnitude (Fig. 1g). Similar observations were made using the human *E. coli* strain Nissle 1917 (Fig. 1h, Extended Data Fig. 3a–b) and a murine *E. cloacae* strain (Fig. 1i, Extended Data Fig. 4a–b). Furthermore, the Adherent Invasive *E. coli* (AIEC) strain NRG857c, originally isolated from a patient with inflammatory bowel disease (IBD), outcompeted the isogenic Δ*moaA* mutant in the intestinal content of DSS-treated mice (Fig. 1j). Tungstate administration negated the fitness advantage conferred by MoCo-biosynthesis and reduced NRG857c colonization (Fig. 1j and Extended Data Fig. 1c and 4c). Similarly, tungstate treatment decreased intestinal colonization of the murine AIEC strain NC101 in a piroxciam-accelerated *Il10*$^{-/-}$ colitis model (Fig. 1k). Taken together, these experiments based on bacterial model organisms indicated that orally-administered tungstate inhibits the MoCo-dependent bloom of Enterobacteriaceae in murine models of colitis.

We next investigated the impact of tungstate treatment on the microbiota. C57BL/6 mice naturally harboring endogenous Enterobacteriaceae (purchased from Charles River Laboratories) were treated with DSS, DSS+tungstate, tungstate alone or were mock-treated. After 9 days, DNA extracted from the cecal content was subjected to shotgun metagenomic sequencing and 16S profiling (Fig. 2 and Extended Data Fig. 2b). Intestinal inflammation was accompanied by significant changes in the predicted coding capacity of the microbiota (Fig. 2a). As we have reported in a recently published metagenomic analysis of the mock- and DSS-treated animals[11], MoCo-dependent processes such as nitrate respiration, trimethylamine *N*-oxide respiration, and formate oxidation were overrepresented[11] (Fig. 2b, Extended Data Fig. 5a). Tungstate administration during colitis abolished these alterations in the metagenome (Fig. 2b and Extended Data Fig. 5a). Mirroring the changes in the coding capacity, tungstate treatment during DSS colitis significantly shifted the microbial community profile from a dysbiotic state towards the normal state (Fig. 2c–e and Extended Data Fig. 5b). Consistent with the idea that MoCo-dependent processes contribute to the inflammation-associated bloom of *E. coli* and other Enterobacteriaceae, tungstate administration selectively blunted the expansion of the Enterobacteriaceae population while other major taxonomic families were only marginally affected (Fig. 2e–g and Extended Data Fig. 5c).

In the absence of inflammation, tungstate treatment did not affect the coding capacity, diversity, community structure, nor the native Enterobacteriaceae population (Fig. 2c, e, and f and Extended Data Fig. 5b–c and 6a). Obligate anaerobic commensals such as *Bacteroides* spp. perform a rudimentary form of anaerobic respiration by reducing endogenous fumarate to succinate. The *Bacteroides* fumarate reductase is not predicted to contain a MoCo binding site and tungstate treatment had no significant impact on the prevalence of predicted fumarate reduction pathways in the microbiome (Extended Data Fig. 6b). Furthermore, tungstate treatment *in vivo* did not affect butyrate production pathways, a major metabolic function of the microbiota (Extended Data Fig. 6c). Supplementation of growth media with tungstate did not inhibit bacterial growth or production of succinate and butyrate by *Bacteroides* and *Clostridium* strains *in vitro* (Extended Data Fig. 6d–h). No overt negative

effects of tungstate on the host were noted (Extended Data Fig. 7). Collectively, these experiments support the idea that tungstate inhibits the inflammation-associated changes in gut microbiota composition that are driven by MoCo-dependent metabolic pathways, in particular the inflammation-associated expansion of the Enterobacteriaceae population.

We then explored the consequences of tungsten-mediated microbiota editing on mucosal inflammation in the DSS colitis model. We analyzed pathological changes, colon length, mRNA levels of pro-inflammatory makers in the cecum and proximal colon, as well as animal body weight in mice harboring endogenous Enterobacteriaceae in the DSS colitis model. Mice experimentally colonized with *E. coli* strains K-12, Nissle 1917, *E. cloacae* or AIEC NRG857c were analyzed in a similar manner. Administration of tungstate significantly reduced inflammatory markers and pathological changes in the large intestinal mucosa, rescued the inflammation-associated reduction of colon length, and ameliorated body weight loss (Fig. 3a–c, Extended Data Fig. 2c–l, 3c–h, 4d–h). This was not due to reduced DSS intake during treatment (Extended Data Fig. 8a). Similarly, tungstate administration in a piroxicam-accelerated *Il10*$^{-/-}$ colitis model reduced intestinal inflammation (Fig. 3d–g). These findings raised the possibility that tungsten-mediated manipulation of the gut microbiota positively affected gut inflammation. Alternatively, one could hypothesize that tungstate exhibited anti-inflammatory effects directly on the host immune system. To test the latter hypothesis, we treated groups of germ-free C57BL/6 mice with DSS and tungstate as well as DSS alone for 9 days and analyzed intestinal inflammatory responses. DSS treatment of germ-free mice resulted in moderate inflammation compared to germ-free control mice. Most importantly, concomitant administration of tungstate did not interfere with the induction of this response, indicating that tungsten limits intestinal inflammation by manipulating the gut microbiota (Fig. 3a–c and Extended Data Fig. 2c–d). No effects of tungstate on pro-inflammatory responses or cellular resistance to DSS injury in tissue culture were observed (Extended Data Fig. 8b–d). Therapeutic administration of tungstate after the onset of inflammation was sufficient to inhibit MoCo-dependent processes in Nissle 1917 (Extended Data Fig. 8e–f), supporting the idea that the effect of tungsten on microbial populations is not due to tungstate interfering with the induction of DSS-induced inflammation. Collectively, these data suggest that tungsten limits gut inflammation through manipulation of the murine gut microbiota.

A subset of IBD patients exhibit changes in their gut microbiota composition, including an increased abundance of Enterobacteriaceae family members[1]. We humanized germ-free mice with gut microbiota from patients with active flares. To model intestinal inflammation, groups of mice were treated with either DSS or DSS+tungstate and housed separately. Administration of tungstate significantly reduced the intestinal Enterobacteriaceae load and decreased markers of mucosal inflammation (Extended Data Fig. 4i–m), thus providing evidence that the effect of tungsten is not unique to the murine microbiota.

An imbalance in the gut-associated microbial community may underlie many human diseases, but current approaches to treat dysbiosis lack the sophistication needed to restore a balanced community *in situ*. Administration of antibiotics broadly reduces numbers of many members of the gut microbiota without discriminating between beneficial and potentially harmful microbes. In some instances, removal of potentially harmful members of the

community can lead to a beneficial outcome[14,15,16]. However, removal of beneficial microbes can lead to pathogen expansion[2,17] or increase bowel irritability[18], thereby adversely effecting the host. Commensal Enterobacteriaceae contribute to colonization resistance against enteric pathogens by competing for critical nutrients[19,20]. Oral administration of probiotic *E. coli* Nissle 1917 is effective in maintaining remission in ulcerative colitis patients[21] and microcins produced by Nissle 1917 suppress the growth of pathogenic bacteria[22]. As such, it might not be desirable to remove commensal Enterobacteriaceae from the ecosystem, but rather control their population size. In contrast to broad-spectrum antibiotics, tungstate treatment of the dysbiotic microbiota allows for the selective control of bacterial populations that rely of MoCo-dependent processes such as Enterobacteriaceae. Since these MoCo-dependent processes are only operational during gut inflammation[11], tungsten treatment only acts on the enterobacterial population during disease and does not eliminate Enterobacteriaceae from the ecosystem during homeostatic conditions. Our work identifies MoCo-dependent processes as a target to control disease-specific aspects of the microbiota composition. Furthermore, our results provide experimental evidence that this rationally-designed microbiome editing approach allows for the improvement of dysbiosis-associated mucosal inflammation.

## Methods

### Bacterial strains

The *E. coli*, *Proteus*, and *E. cloacae* strains used in this study are listed in Supplementary Table 1. All strains were routinely grown aerobically in LB broth (10 g/l tryptone, 5 g/l yeast extract, 10 g/l NaCl) or on LB agar plates (10 g/l tryptone, 5 g/l yeast extract, 10 g/l NaCl, 15 g/l agar) at 37°C. When appropriate, antibiotics were added to the media at the following concentrations: 30 μg/ml chloramphenicol (Cm), 100 μg/ml carbenicillin (Carb), 50 μg/ml kanamycin (Kan).

### Plasmids

All the primers and plasmids used in this study are listed in Supplementary Table 2 and Supplementary Table 3. pWZ5 was constructed using standard molecular cloning techniques[23] and the Gibson Assembly Cloning Kit (New England Biolab, Boston) according to the recommendations of the manufacturer. The flanking regions of the NRG857c *moaA* gene were amplified and ligated into pGP706 to give rise to pWZ5. Plasmid inserts were verified by Sanger sequencing.

### Construction of mutants by allelic exchange

pWZ5 was propagated in DH5α λ*pir* and conjugated into the *E. coli* strains NRG857c or NC101 via using S17-1 λ*pir* as the conjugative donor strain. Exconjugants that had the suicide plasmid integrated into the recipient chromosome (single crossover) were recovered on LB plates containing appropriate antibiotics. Sucrose plates (8 g/l nutrient broth base, 5 % sucrose, 15 g/l agar) were used to select for the second crossover event, thus creating WZ12 and WZ245, respectively. Deletion of the target gene was confirmed by PCR.

### Anaerobic growth assays

Anaerobic growth assays were performed in mucin broth. Mucin broth contained hog mucin (Sigma-Aldrich, St. Louis) at a final concentration of 0.5 % (w/v) in no-carbon E medium[24] and was supplemented with trace elements[25]. Sodium formate, sodium nitrate, DMSO and TMAO (Sigma Aldrich, St. Louis) were added at a final concentration of 40 mM, in the absence or presence of sodium tungstate (Sigma Aldrich) at the indicated final concentrations. A volume of 2 ml of mucin broth was inoculated with the indicated strains at a concentration of $1 \times 10^4$ colony forming units (CFU)/ml and incubated anaerobically (Bactron EZ Anaerobic Chamber; Sheldon Manufacturing) for 18 h at 37°C. Bacterial numbers were numerated as described[12].

### DSS colitis model and sodium tungstate treatment

All experiments involving mice were approved by the Institutional Animal Care and Use Committee at UT Southwestern Medical Center (APN#T-2013-0159) and UC Davis (APN#16196). Studies involved animals were performed with compliance to all relevant ethical regulations. Female 9–12 week old C57BL/6J wild-type mice were obtained from the Jackson Laboratory (Bar Harbor) and bred at UT Southwestern (essentially devoid of endogenous Enterobacteriaceae) or Charles River Laboratories (Morrisville) (harboring endogenous Enterobacteriaceae), as indicated. Mice were randomly assigned into cages before the experiment. The drinking water was replaced with either filter-sterilized water (mock-treatment), or a filter-sterilized solution of 0.2% (w/v) sodium tungstate (Sigma, St Louis), or a filter-sterilized solution of 2% or 3% (w/v) dextran sulfate sodium (DSS; relative molecular mass 36,000 – 50,000; MP Biomedicals) in water at the indicated concentrations, or a filter-sterilized solution of DSS and 0.2% (w/v) sodium tungstate. In one experiment, tungsten was administered in a sodium tungstate-fortified diet (1000 ppm). At the indicated time points, animals were orally inoculated with either 0.1 ml of LB broth or 0.1 ml LB broth containing $1 \times 10^9$ CFU *E. coli*, or remained uninfected. In the competitive colonization experiments, animals were inoculated with $5 \times 10^8$ CFU of each *E. coli* or *E. cloacae* strain. One day prior to the end of the experiment, the drinking water was switched for 24 h to regular, filter-sterilized water to reduce the amount of DSS present in the samples. After euthanization, colonic and cecal tissue were collected, flash frozen and stored at −80°C for subsequent mRNA and protein expression analysis. Fecal material, cecal content, and colonic content were harvested in sterile PBS and the bacterial load for the *E. coli* strains or Enterobacteriaceae was numerated by plating serial 10-fold dilutions on LB plates supplemented with appropriate antibiotic or MacConkey Agar plates, respectively. *E. coli* NC101 and Nissle 1917 strains were differentially marked with the low-copy number plasmids pWSK29 and pWSK129 to facilitate bacterial recovery from biological samples[12]. For the competitive colonization experiments involving NRG857c, animals were inoculated with an equal mixture of the NRG857c Δ*lacZ* mutant (LB33) and the Δ*moaA* mutant (WZ12) as described above. The bacterial load in the luminal content of the indicated organs was determined by plating serial 10-fold dilutions on LB plates supplemented with the appropriate antibiotics and 40 mg/l 5-bromo-4-chloro-3-indolyl-β-D-galactopyranoside. Germ-free C57BL/6 mice were maintained in plastic gnotobiotic isolators on a 12-hour light cycle. DSS-mediated colitis was induced in 8–12 week old germ-free mice, following the protocol described above.

### Piroxicam-accelerated colitis model in conventional *Il10*$^{-/-}$ mice

Conventional *Il10*$^{-/-}$ mice on C57BL/6 (7–12 weeks, males only) backgrounds were randomly assigned into cages before orally inoculated with $1 \times 10^9$ CFU of mouse AIEC NC101. Regular mouse chow was replaced with Piroxicam-fortified diet (100 ppm; Teklad custom research diets, Envigo) and changed daily. Drinking water was either replaced with filter-sterilized water (mock) or a filter-sterilized solution of 0.2% (w/v) sodium tungstate. After 14 days, mice were euthanized and the samples were collected as described above.

### Fecal transplant into gnobiotic mice

All procedures involving human subjects were reviewed and approved by the institutional review board at the University of Texas Southwestern Medical Center (IRB#112010-130). Studies involved human samples were performed with compliance to all relevant ethical regulations. Written informed consent was obtained from all participants or parents/legal guardians of participating minors. Except for the study PI and study coordinator (Burstein and Sifuentes-Dominguez), all study personnel handling these samples did not have access to personal identification information. Patients were considered for fecal donation if they had an established diagnosis of inflammatory bowel disease, had active disease at the time of collection and were free from antibiotic use over the past 3 months. Patient characteristics from samples used are summarized in Supplementary Table 4. Human fecal samples were obtained at time of colonoscopy by direct endoscopic aspiration of fecal contents from patients with active colonic disease. A total of 10ml of liquid fecal material was collected from each patient and aliquoted into 1ml cryovials. The samples were then snap frozen in liquid nitrogen and stored at −80°C until used.

Germ-free Swiss-Webster mice (7–12 weeks, mix of male and female) were maintained in plastic gnotobiotic isolators on a 12-hour light cycle. Mice were randomized, paired and orally gavaged with endoscopy samples from the patients listed in the table at the end of this section. The colonization was allowed to proceed for 3 days before mice receiving DSS or DSS plus sodium tungstate for 7 days. Mice were euthanized and the samples were collected as described above.

### 16S RNA pyrosequencing and analysis

Cecal contents was collected and the DNA was extracted from fecal samples using the MoBio PowerFecal kit (MoBio Laboratories, Carlsbad.) according to the recommendations of the manufacturer. The extracted DNA was subjected to KCl precipitation to remove residual DSS contaminants. Briefly, DNA was incubated with excess amount of KCl on ice to precipitate DSS. The samples were then cleared by centrifugation and the resulting supernatant was subsequently subjected to ethanol precipitation to recover the DNA. The purified DNA was subjected to paired end (PE) library construction to facilitate assemblies and longer accurate reads. The 16S rRNA coding sequences used to identify the bacteria were amplified using primers 515F and 806R that flank the V3–V4 hypervariable region, and barcoded prior to pyrosequencing. The barcoded amplicons were purified and quantified on an Invitrogen Qubit system (Life technology, OR). Libraries were sequenced using an Illumina MiSeq system (Illumina, CA). 16S sequencing data was subjected to a standard workflow for processing and quality assessment of the raw 16S sequence data and the

downstream phylogenetic analysis. The pipeline consists of an initial customized Linux-based command script for trimming, demultiplexing, and quality filtering the raw PE sequence data generated by Illumina system. Sequence alignment, operational taxonomic units (OTUs) picking against the Greengenes reference collection, clustering, phylogenetic and taxonomic profiling, permanova analysis, and the analysis of beta diversity (principle component analysis) on the demultiplexed sequences were performed with the Quantitative Insights into Microbial Ecology QIIME open source software package[26].

## Metagenomics

Groups of randomized Charles River C57BL/6 were treated as described in Extended Data Fig. 2b. Sample collection, shotgun metagenomics sequencing and data analysis were performed as previously described[11].

In this study, reads mapped to the SEED database were exported from MEGAN5 into BIOM tables, which were subjected to Analysis of similarity (ANOSIM) in Qiime[26] and Principle Component Analysis (PCA) using STAMP[27]. To map reads to bacterial metabolic genes, a total of 100 each of the butyrate production operons (*bcdAB, but* and *ato*) and succinate dehydrogenase operon (*sdhABC*) were downloaded from the KEGG database. Sequences were clustered to remove redundancy using cdhit-est[28,29] with a sequence identity threshold of 0.9. Paired end reads were mapped to these gene clusters using the BBmap tool with the following settings: qtrim=lr, minid=0.90, ambig=random, covstats=true. Coverage statistics for each gene cluster were tallied from the percent unambiguous and ambiguous mapped reads and used to determine the absolute number of reads that mapped to a particular gene set. A similar strategy was used to map reads to fumarate respiration and butyrate production pathways.

## Abundance of *Enterobacteriaceae*

The relative abundance of endogenous *Enterobacteriaceae* as part of the bacterial microbiota was analyzed as described previously[30–32]. Briefly, the cecum or colon content was extracted using The PowerFecal DNA Isolation Kit (MoBio Laboratories, Carlsbad) per manufacturer's instructions, and the resulting DNA was further purified using the KCl method as described above. A 2 μl sample of the bacterial DNA was used as the template for SYBR-green based real-time PCR reactions as described above. The gene copy number in the sample was determined based on a standard curve generated by using pSW321 and pSW196 as previously described[33]. The primers used in this experiment were listed in supplementary table 2. The fraction of *Enterobacteriaceae* as part of the entire bacterial population for each sample was calculated by dividing the gene copy number of the *Enterobacteriacaea* by the gene copy number determined using the eubacterial primers.

## Quantification of mRNA levels in intestinal tissue

The relative transcription levels of iNOS, CXCL1 (Kc), CXCL2, IL-17, IL-6, IFN-γ, Lcn2 and TNF-α, encoded by the *Nos2*, *Cxcl1*, *Cxcl2, Il17, Il6*, *Ifng*, *Lcn2* and *Tnf* genes, respectively, was determined by qRT-PCR as described previously[31]. Briefly, colonic or cecal tissue was homogenized in a Mini beadbeater (Biospec Products, Bartlesville) and RNAs were extracted using the TRI reagent method (Molecular Research Center,

Cincinnati). To remove residual DSS contaminants, RNA was further purified using the Dynabeads mRNA Direct Kit (Life Technologies) per the manufacturer`s instructions. cDNA was generated by TaqMan reverse transcription reagents (Life Technologies). Real-time PCR was performed using SYBR Green (Life Technologies) and data was acquired in a QuantStudio 6 Flex instrument (Life Technologies) and analyzed using the comparative Ct method. The primers listed in Supplementary Table 2 were added at a final concentration of 250 nM. Target gene transcription of each sample was normalized to the respective levels of *Gapdh* mRNA.

## Histopathology

Murine cecal and colonic tissue was fixed in phosphate-buffered formalin and 5 μm sections of the tissue were stained with hematoxylin and eosin. The fixed and stained sections were blinded and evaluated by an experienced veterinary pathologist according to the criteria as described previously[12]. Images were taken at a magnification of 10 ×, and the contrast for the images was uniformly (linear) adjusted using Photoshop CC.

## Measurement of succinate and butyrate concentrations in bacterial culture using GC-MS

Bacterial cultures were cleared by first centrifuging at 13,200 g at 4 °C for 30 minutes and passing through a 0.22 μm filter. The supernatant was dried using a SpeedVac concentrator. The pellet was then dissolved in pyridine at 80 °C for 20 mins before derivatization with *N*-*tert*-Butyldimethylsilyl-*N*-methyltrifluoroacetamide with 1 % t-BDMCS (Cerilliant) at 80 °C for 1h. Derivatized samples were transferred to autosampler vials for gas chromatography-mass spectrometry (GC-MS) analysis (Shimadzu, TQ8040). The injection temperature was 250 °C and the injection split ratio was set to 1:100 or 1:1000 with an injection volume of 1 μL. GC oven temperature started at 130 °C for 4 min, rising to 230 °C at 4 °C/min and to 280 °C at 20 °C/min with a final hold at this temperature for 2 min. GC flow rate of the helium carrier gas was kept constant at a linear velocity of 50 cm/s. The column used was a 30 m × 0.25 mm × 0.25 μm Rtx-5Sil MS (Shimadzu). The interface temperature was 300 °C. The electron impact ion source temperature was 200 °C, with 70 V ionization voltage and 150 μA current. To measure succinate, Q3 scans (range of 50–500 m/z, 1000 m/z per second) were first performed to determine the retention time for succinate and succinate-2,2,3,3-$d_4$ (CDN Isotopes), which was 11.0 and 10.9 minutes respectively. Multiple reaction monitoring mode was then used (target ion m/z 289>147, reference ion m/z 331>189) to quantitatively measure succinate. To measure butyrate, Q3 scans were performed as described above, and the retention time for butyrate and butyrate-$d_7$ (CDN Isotopes) was 6.1 and 6.2 minutes respectively. Q3 selected ion monitoring (single quadrupole mode) with an event time of 0.05 s was performed to quantitatively measure butyrate. The target and reference (qualifier) ions for butyrate were m/z = 145 and m/z = 75, respectively; target and reference ions for deuterated butyrate were m/z = 152 and m/z = 76.

## Strain isolation and identification

10-fold serial dilutions of the fecal content of C57BL/6 mice (Charles River, Morrisville) were plated on MacConkey medium (10g/l pancreatic digest of gelatin, 3 g/l peptone, 10 g/l lactose, 1.5 g/l bile salts, 5 g/l sodium chloride, 13.5 g/l agar, 30 mg/l neutral red, 1 mg/l crystal violet) and incubated aerobically at 37°C overnight. To isolate murine commensal *E.*

*coli* and *Proteus* strains, single colonies were isolated and subjected to species identification using the EnteroPluri Test (Liofilchem, Italy) per the manufacturer`s recommendations.

### Nitrate reductase activity assays

Overnight cultures of *E. coli* or *Proteus* strains were diluted 1:100 in fresh LB broth containing 40 mM sodium nitrate to induce the expression of nitrate reductases, in the presence of absence of sodium tungstate at the indicated concentrations. Cultures were aerobically incubated for 3 h at 37°C and the relative nitrate reductase activity was measured as described previously[34]. The experiment was repeated 3 times and the representive results were shown.

### NF-κB activation in epithelial cells

HeLa57A cells, stably transfected with an NF-κB-luciferase reporter construct[35,36], were maintained in Dulbecco's modified Eagle's medium containing 10 % fetal calf serum at 37°C in a 5 % $CO_2$ atmosphere. For the NF-κB activation assays, cells were seeded in a 48 well plate to reach 80 % confluency within 24 hours. Cells were treated with 0.1, 1, or 10 ng/ml of PMA (dissolved in DMSO) or DMSO. At the same time, sodium tungstate with a final concentration of 0.02 % or 0.002 % (w/v/) in water was added to the cells. After 5 hours, cells were washed in DPBS and lysed in 0.1 ml of reporter lysis buffer (Promega). Firefly luciferase activity was measured with a commercial luciferase assay system (Promega). The experiment was repeated 3 times and the representive results were shown.

### LDH Release Assay

The MODE-K cell line was maintained in Dulbecco's Modified Eagle Medium (DMEM; Sigma) supplemented with 10 % FBS at 37°C in 5 % $CO_2$. Bone-marrow-derived macrophages (BMDMs) were differentiated from bone marrow cells collected from femurs and tibias of SPF C57BL/6 mice. Briefly, bone marrow cells were harvested with 10 ml of cold RPMI-1640 medium (Sigma) and then pelleted at 1,000 rpm for 5 min at 25 °C. The cells were re-suspended in BMM medium (RPMI-1640 supplemented with 10 % heat-inactivated FBS, 1 mM glutamine, 1% antibiotics-antimycotics, and 30 % L-cell conditioned medium) and allowed for differentiation for 7 days. MODE-K experiments were performed in triplicate. Plates were seeded with cells to a final confluency of 80 % before treatment. Two days after seeding, MODE-K cells were treated for 24 h with 2–4 % DSS (Alfa Aesar), with and without 0.002–0.2 % sodium tungstate dihydrate (Sigma). For BMDM experiments, plates were seeded with $1\times10^5$ cells per well for 48 h. After 24h the media was replaced to RPMI supplemented with 2 % FBS and glutamine. On the day of the experiment, culture media was replaced with media supplemented with 4 or 6 % DSS, with and without 0.2% sodium tungstate dehydrate, for 24 h. Cytotoxicity was determined using the LDH release assay CytoTox 96 Non-Radioactive Cytotoxicity Assay (Promega), per the manufacturer's recommendations. Absorbance readings were corrected based on the absorbance of the medium alone. Five-minute treatment with 10 % Triton X-100 was used as the total LDH release control. The experiment was repeated 3 times and the representive results were shown.

### Statistical and reproducibility

Nitrate reductase activities, fold changes in mRNA levels, competitive indices, relative abundance of *Enterobacteriaceae*, and bacterial numbers underwent logarithmic transformation and the statistical significance of differences between groups was determined using a two-sided Student's *t*-test or permutational multivariate analysis of variance (using distance matrices) (permanova) analysis. Cumulative histopathology scores were analyzed using the Mann-Whitney *U*-test. Details regarding the statistics of each experiment are reported in Supplementary Table 5.

### Data availability statement

The bacterial 16S rDNA and metagenomics sequencing reads generated and analysed during the current study are available at the European Bioinformatics Institute repository under accession numbers PRJEB15095 and PRJEB19192. All data generated or analysed during this study are included in this published article (and its supplementary information files).

## Extended Data

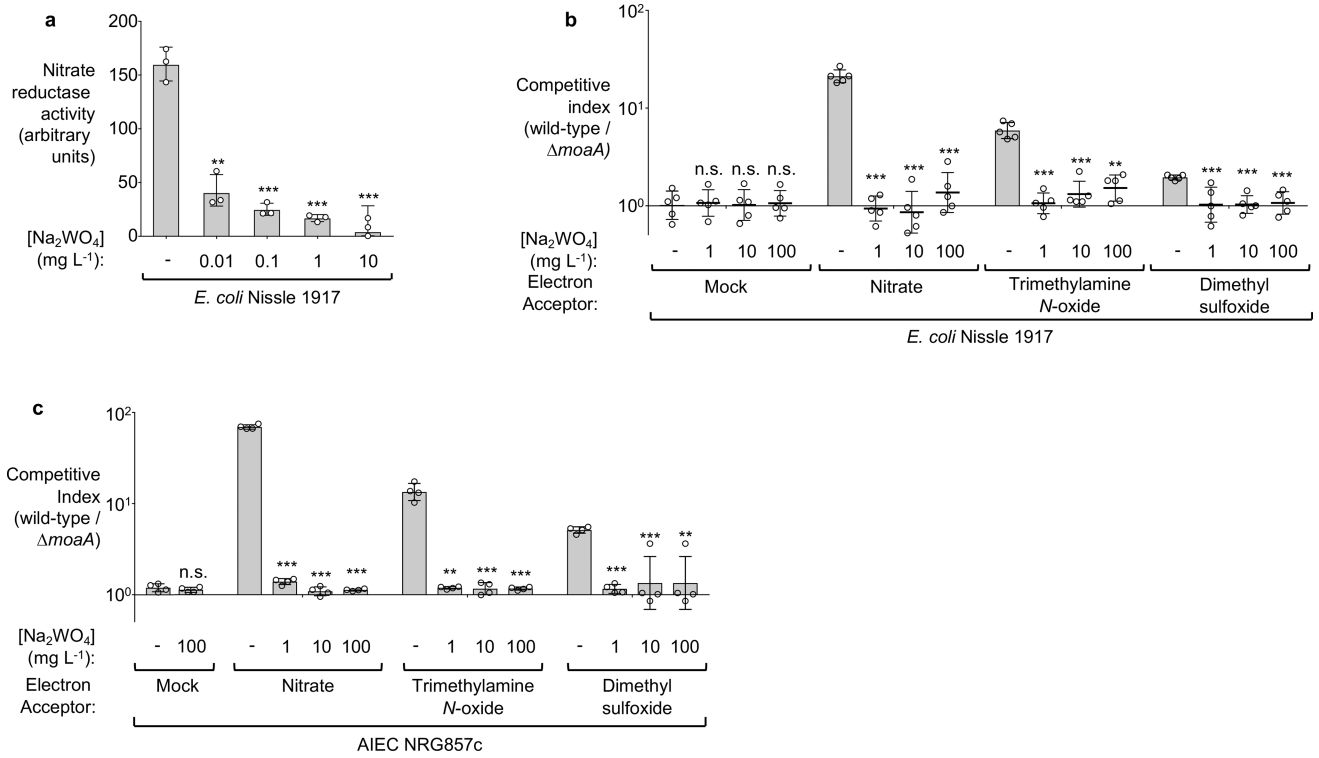


**Extended Data Figure 1. Effect of tungstate on anaerobic respiration *in vitro***

**a**, Nitrate reductase activity of *E. coli* Nissle 1917 measured in media supplemented with sodium nitrate and the indicated concentrations of sodium tungstate. **b,** Competitive growth of the *E. coli* Nissle 1917 wild-type strain and the isogenic molybdenum cofactor-deficient mutant (*moaA*) in the presence of the indicated electron acceptors under anaerobic conditions. **c,** Competitive growth of *E. coli* NRG857c wild-type strain and the isogenic

molybdenum cofactor-deficient mutant (*moaA*) in the presence of the indicated electron acceptors under anaerobic conditions. **a–c,** $n$=3 replicates per condition. $n$ denotes the number of biological replicates. Bars represent the geometric mean of three experiments ± geometric standard deviation. **, $P < 0.01$; ***, $P < 0.001$; ns, not statistically significant compared to media containing no sodium tungstate.

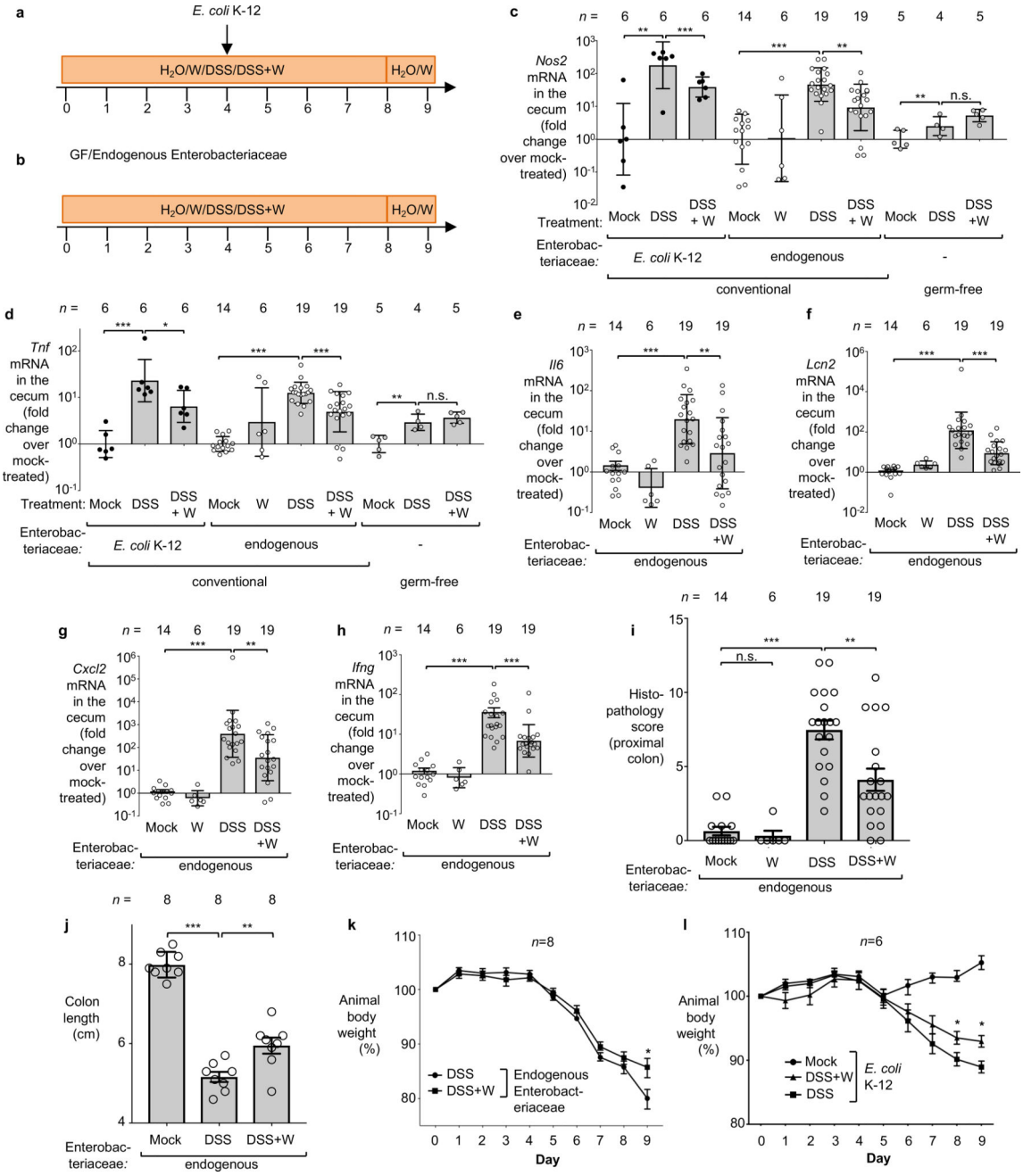


**Extended Data Figure 2. Tungstate treatment of mice colonized with *E. coli* K-12**

Conventionally-raised C57BL/6 mice were treated with 0.2 % sodium tungstate (W), dextran sulfate sodium (DSS), DSS+W, or left untreated (mock). After 4 days, animals were orally

inoculated with the *E. coli* K-12 wild-type strain and the isogenic *moaA* mutant. C57BL/6 mice with naïve microbiota (endogenous Enterobacteriaceae only) or germ-free C57BL/6 mice were similarly treated but were not inoculated with *E. coli* indicator strains. Samples were analyzed after a total of 9 days of treatment. **a–b,** Schematic representation of the colitis models used in this figure. **c–h** Transcription of *Nos2* (**c**), *Tnf* (**d**), *Il6* (**e**), *Lcn2* (**f**), *Cxcl2* (**g**) and *Ifng* (**h**) in the cecal mucosa was determined by RT-qPCR, *E. coli* K-12: $n$=6 per group; Endogenous Enterobacteriaceae, Mock ($n$=14), W ($n$=6), DSS ($n$=19), DSS+W ($n$=19); Germ-free: Mock ($n$=5), DSS ($n$=4), DSS+W ($n$=5). **i**, Cumulative histopathology score for the colon tissue, Mock ($n$=14), W ($n$=6), DSS ($n$=19), DSS+W ($n$=19); bars represent means ± standard error and each dot represents one animal. **j**, Colon length, $n$=8 per group. **k**, Body weight of mice harboring endogenous Enterobacteriaceae, $n$=8 per group. **l,** Body weight of mice experimentally colonized with *E. coli* K-12, $n$=6 per group. Unless noted otherwise, bars represent the geometric mean ± geometric standard deviation. *, $P < 0.05$; **, $P < 0.01$; ***, $P < 0.001$. n.s., not significant.

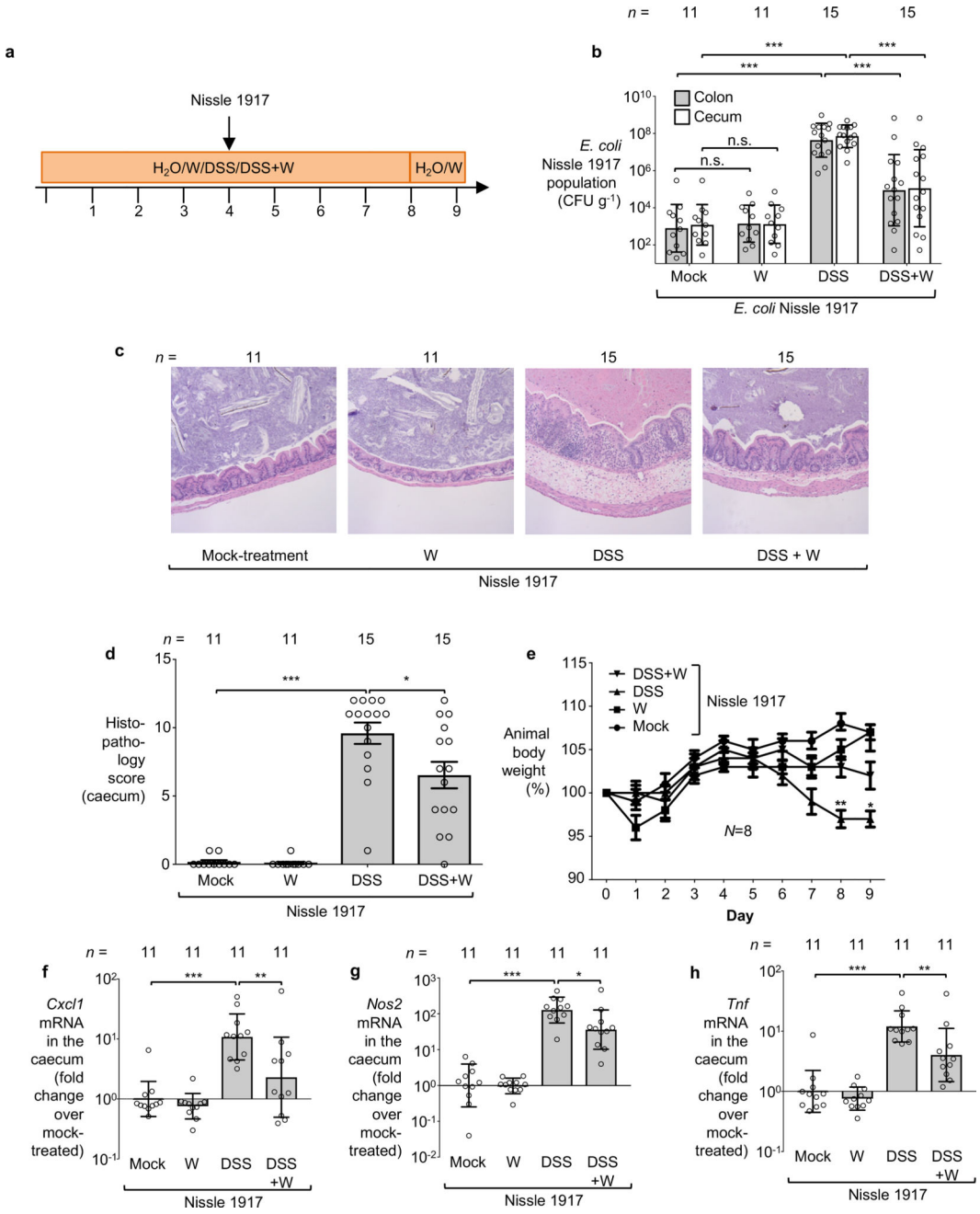


**Extended Data Figure 3. Impact of tungstate treatment on mice experimentally colonized with *E. coli* Nissle 1917**

Groups of conventionally-raised C57BL/6 mice were orally inoculated with the *E. coli* Nissle 1917 wild-type strain and treated with 0.2 % sodium tungstate (W), dextran sulfate sodium (DSS), DSS and sodium tungstate, or left untreated (mock) for 9 days. **a,** Schematic representation of colitis model used in this figure. **b**, Bacterial load in the cecum (white bars) and colon content (black bars). **c–d** Formalin-fixed, hematoxylin and eosin-stained sections of the cecum were scored for the presence of inflammatory lesions. **c,** Representative images of stained cecal sections. **d,** Cumulative histopathology score for the cecum tissue; bars

represent means ± standard error and each dot represents one animal. **b–d**, Mock and W ($n$=11 per group), DSS and DSS+W ($n$=15 per group). **e,** Animal body weight, $n$=8 per group. **f–h** The transcription of the inflammatory marker genes *Cxcl1* (**f**), *Nos2,* (**g**) and *Tnf* (**h**) in the cecal mucosa was determined by RT-qPCR, $n$=11 per group.
Unless noted otherwise, bars represent the geometric mean ± geometric standard deviation. *, $P < 0.05$; **, $P < 0.01$; ***, $P < 0.001$. n.s, not significant.

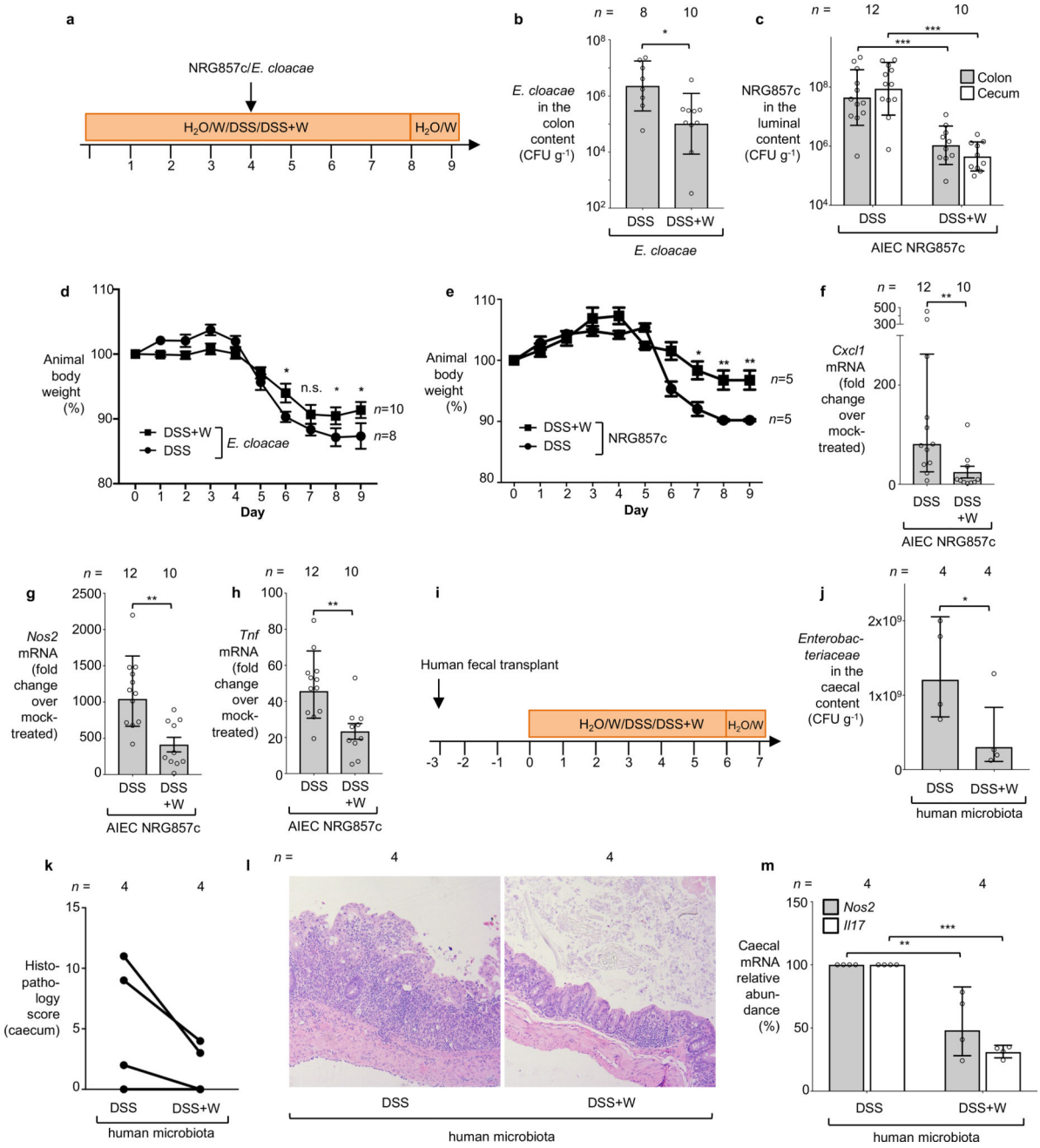


**Extended Data Figure 4. Effect of tungstate treatment on mice experimentally colonized with *Enterobacter cloacae* and Adherent Invasive *E. coli***

**a–h,** Conventionally-raised C57BL/6 mice were treated with DSS or DSS+W. After 4 days, animals were intragastrically inoculated with the indicated bacterial strains. Samples were collected 5 days after inoculation. **a**, Schematic representation of the experiments. **b** and **c**, The total population of *E. cloacae* (**b**) and NRG857c (**c**) in the large intestinal content was determined by plating on selective media. **d** and **e**, Animal body weight. **b** and **d**, DSS ($n$=8), DSS+W ($n$=10). **c**, DSS ($n$=12), DSS+W ($n$=10). **e,** $n$=5 per group. **f–h** The transcription of the inflammatory marker genes *Cxcl1* (**f**) *Nos2* (**g**), and *Tnf* (**h**) in the cecal mucosa was determined by RT-qPCR, DSS ($n$=12), DSS+W ($n$=10). **i–m**, Paired germ-free Swiss-Webster mice received human fecal transplant and were subjected to DSS or DSS + 0.2 % sodium tungstate (W) treatment for 7 days, DSS ($n$=4), DSS+W ($n$=4) **i**, Schematic representation of the experiments. **j,** The abundance of Enterobacteriaceae in the cecal content was determined by plating on selective media (MacConkey agar). **k,** Formalin-fixed, hematoxylin and eosin-stained sections of the murine cecum were scored for the presence of inflammatory lesions. **l,** Representative images of stained murine cecal sections. **m,** The transcription of the inflammatory marker genes *Nos2* and *Il17* in the murine cecal mucosa. Bars represent the geometric mean ± geometric standard deviation. *, $P < 0.05$; **, $P < 0.01$; ***, $P < 0.001$. n.s, not significant.

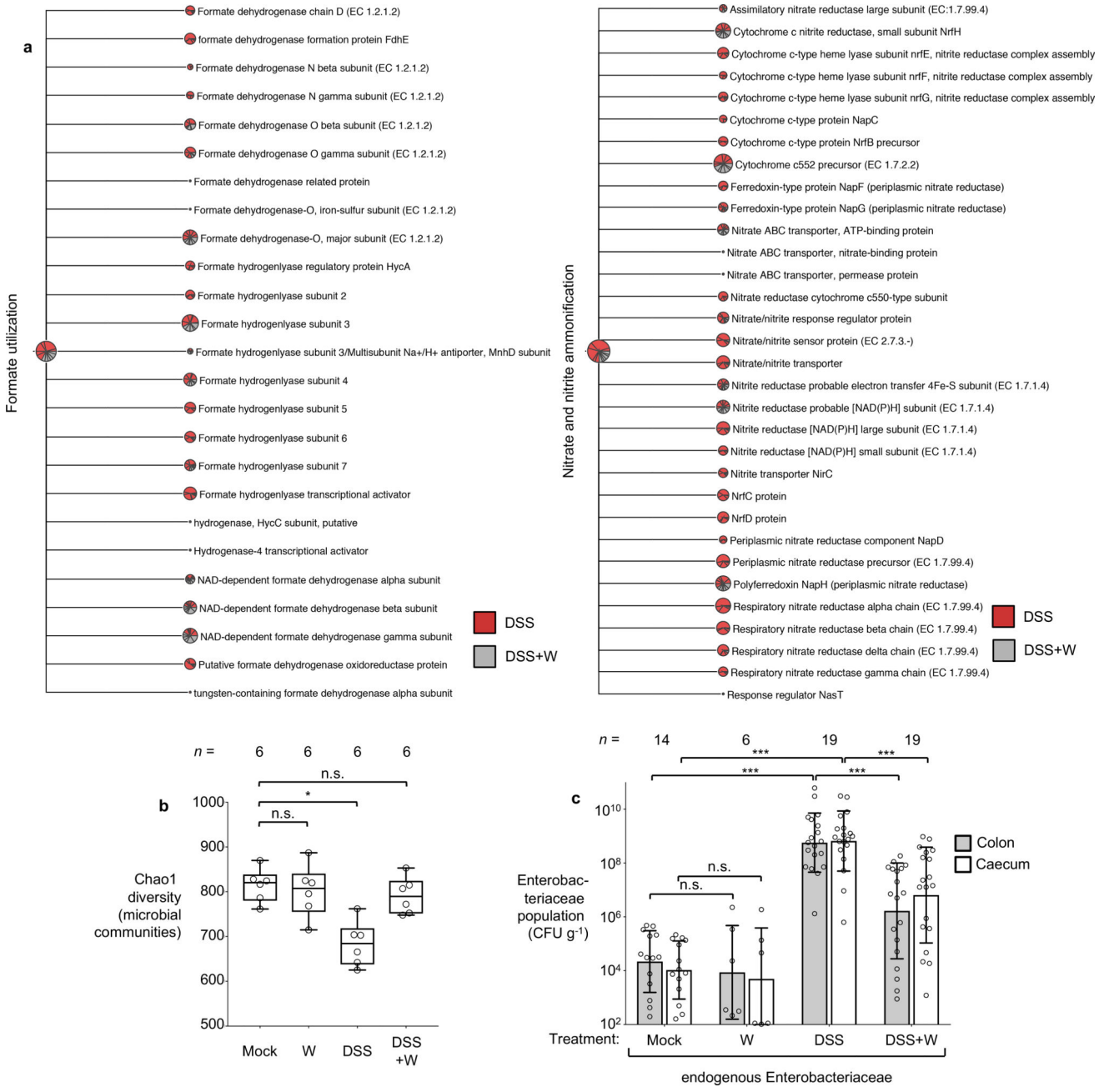


**Extended Data Figure 5. Impact of tungstate on the naïve gut microbiome**

Groups of C57BL/6 mice naturally harboring Enterobacteriaceae were treated with 0.2 % sodium tungstate (W), dextran sulfate sodium (DSS), DSS+W, or left untreated (mock) for 9 days (see also Extended Data Fig. 3b). **a,** Relative abundance of genes involved in formate and nitrate utilization in the cecal content revealed by shotgun metagenomic sequencing (MEGAN5). Each section of the pie chart is representative of the number of reads mapped obtained for the individual animals ($n$=6 per group). **b,** Box-and-whisker plot (Min to Max) of Chao1 alpha diversity of the cecal microbiota community based on 16S profiling ($n$=6 per group). **c,** Abundance of endogenous Enterobacteriaceae family members determined by

plating on selective media (MacConkey agar), Mock ($n$=14), W ($n$=6), DSS ($n$=19), DSS+W ($n$=19).

Bars represent the geometric mean ± geometric standard deviation. *, $P < 0.05$; ***, $P < 0.001$. n.s., not significant.

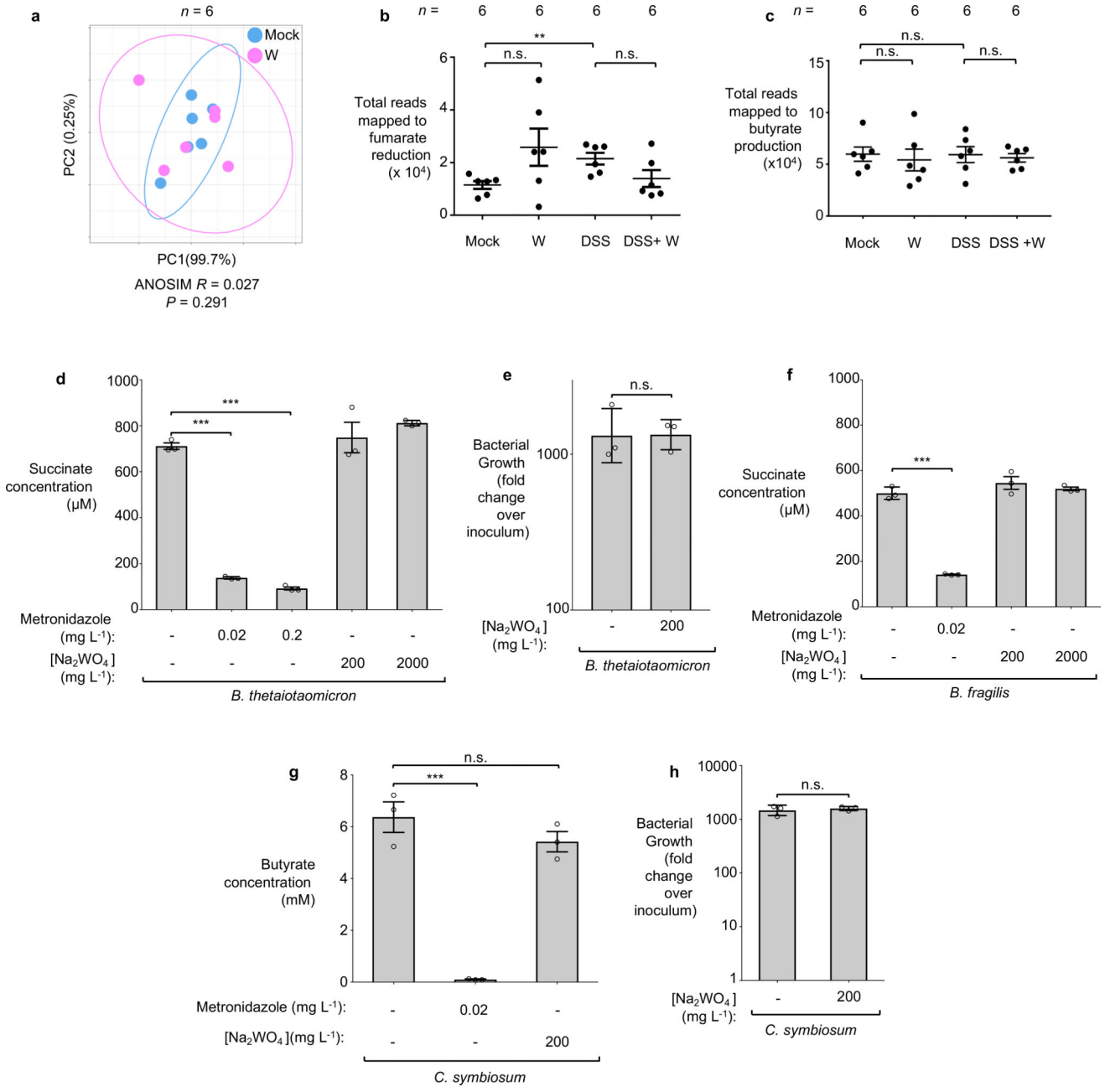


**Extended Data Figure 6. Effect of tungstate treatment on obligate anaerobic commensal bacteria**

**a–c** Metagenomic analysis of the cecal content of mice described in Extended Data Fig. 3b. **a,** Principal coordinates (PC) analysis of global metabolic pathway and quantification of reads involved in fumarate respiration (**b**) and butyrate production (**c**). Ellipses in **a** denotes 95% confident interval. Bars represent the mean of ± standard deviation. **a–c**, $n$=6 per group.

**d–f** *B. thetaiotaomicron* or *B. fragilis* were cultured anaerobically in mucin broth at 37 °C for 48 hours. Media was supplemented with sodium tungstate or metronidazole as indicated. Succinate production by *B. thetaiotaomicron* (**d**) and *B. fragilis* (**f**) was assessed by GC-MS. The growth of *B. thetaiotaomicron* was determined by plating serial dilution of bacterial culture on blood agar (**e**). **g,** *C. symbiosum* was inoculated into chopped meat broth and incubated anaerobically at 37 °C for 36 hours. Butyrate concentration in the media was measured using GC-MS. **h,** *C. symbiosum* was anaerobically cultured in chopped meat broth at 37 °C for 48 hours. The growth of *C. symbiosum* was determined by plating serial dilution of bacterial culture on thioglycolate plates. **d–h,** $n$=3 replicates per condition. Bars represent the geometric mean of three experiments ± geometric standard deviation. **, $P < 0.01$; ***, $P < 0.001$. n.s., not significant.

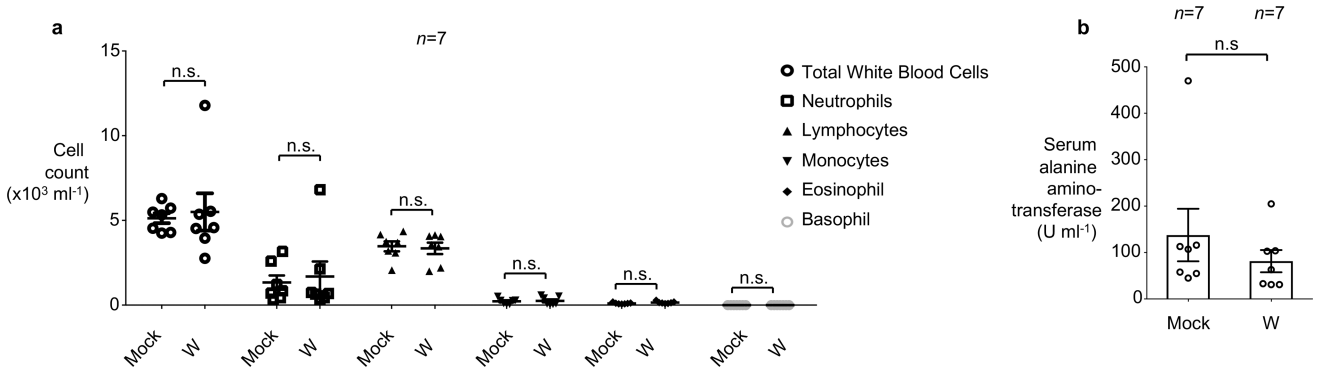


**Extended Data Figure 7. Assessment of overall health of mice orally treated with tungstate**

Groups of seven mice were either mock treated or treated with 0.2 % sodium tungstate (W) in the drinking water for 9 days. **a,** Complete blood count. **b,** Serum alanine amino-transferase concentration. **a–b**, $n$=7 animals per group.

Bars represent the geometric mean ± geometric standard deviation. n.s., not statistically significant.

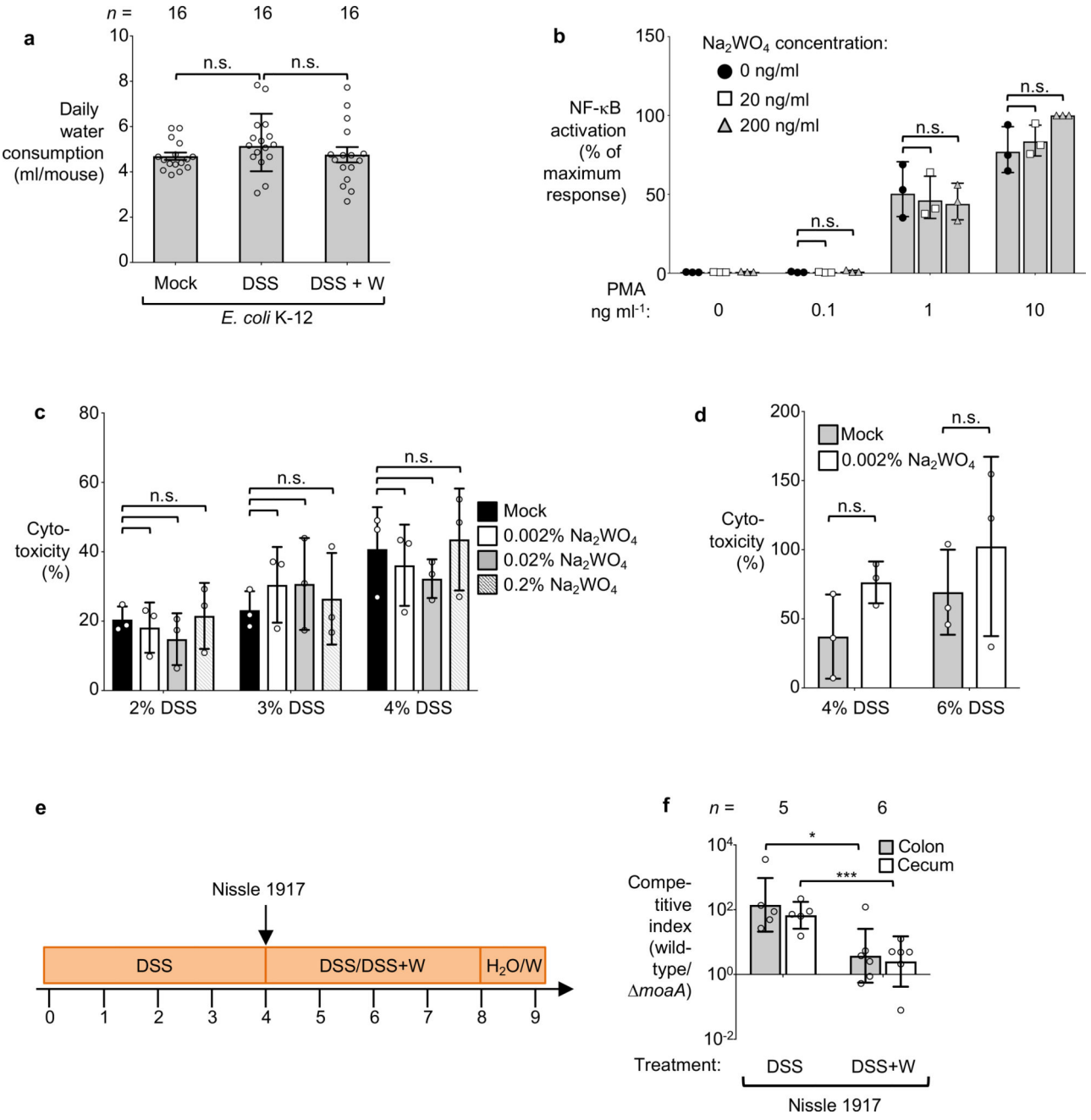


**Extended Data Figure 8. Exposure of tissue culture cells to sodium tungstate**

**a**, Daily water consumption of the *E. coli* K-12 inoculated mice. Each dot represents the average daily water consumption (ml/day) of 3 mice, obtained during 8 time points, with 2 cages per treatment group, *n*=16. **b,** HeLa57A cells, expressing luciferase under control of a NF-κB-dependent promoter, were treated with Phorbol 12-myristate 13-acetate (PMA) and sodium tungstate (W) at the indicated concentrations. Relative luciferase activity was determined after 5 hours. **c–d**, MODE-K or bone marrow derived macrophage (BMDMs) cells were treated with DSS or DSS+sodium tungstate at the indicated concentration for 24 hours. The release of lactate dehydrogenases into the culture supernatant by MODE-K cells

(**c**) or BMDMs (**d**) was measured. **e–f**, Groups of conventionally-raised C57BL/6 mice were treated with DSS for 4 days. Animals were intragastrically inoculated with an equal mixture of the indicated *E. coli* Nissle 1917 wild-type strain and an isogenic *moaA* mutant. On the day of inoculation, a subset of mice was switched to DSS+sodium tungstate (W) for 4 days while a control group remained on DSS treatment. **b–d**, $n$=3 replicates per condition. **e,** Schematic representation of experiment. **f**, The competitive index in the cecal (white bars) and colon content (black bars) was analyzed 5 days after inoculation, DSS ($n$=5), DSS+W ($n$=6).

Bars represent the geometric mean ± geometric standard deviation. *, $P < 0.05$; ***, $P < 0.001$. n.s., not significant.

## Supplementary Material

Refer to Web version on PubMed Central for supplementary material.

## Acknowledgments

This work was supported by NIH grants AI112445 (A.J.B), AI118807 (S.E.W), AI128151 (S.E.W), DK070855 (L.V.H.), DK102436 (B.A.D.), and 5K12HD-068369 (L.S-D.), Welch Foundation grants I-1858 (S.E.W.) and I-1874 (L.V.H), American Cancer Society Research Scholar Grant MPC-130347 (S.E.W.), and a Crohn's and Colitis Foundation of America postdoctoral fellowship #454921 (W.Z.). Work in L.V.H. lab is supported by the Howard Hughes Medical Institute. The funders had no role in study design, data collection and interpretation, or the decision to submit the work for publication. Any opinions, findings, and conclusions or recommendations expressed in this material are those of the author(s) and do not necessarily reflect the views of the funders. We would like to thank Dr. Balfour Sartor for providing the *E. coli* NC101 strain.

## References

1. Frank DN, et al. Molecular-phylogenetic characterization of microbial community imbalances in human inflammatory bowel diseases. Proc Natl Acad Sci U S A. 2007; 104:13780–13785. DOI: 10.1073/pnas.0706625104 [PubMed: 17699621]
2. Lupp C, et al. Host-mediated inflammation disrupts the intestinal microbiota and promotes the overgrowth of Enterobacteriaceae. Cell Host Microbe. 2007; 2:204. [PubMed: 18030708]
3. Garrett WS, et al. Enterobacteriaceae act in concert with the gut microbiota to induce spontaneous and maternally transmitted colitis. Cell Host Microbe. 2010; 8:292–300. DOI: 10.1016/j.chom.2010.08.004 [PubMed: 20833380]
4. Mshvildadze M, et al. Intestinal microbial ecology in premature infants assessed with non-culture-based techniques. J Pediatr. 2010; 156:20–25. DOI: 10.1016/j.jpeds.2009.06.063 [PubMed: 19783002]
5. Vujkovic-Cvijin I, et al. Dysbiosis of the gut microbiota is associated with HIV disease progression and tryptophan catabolism. Sci Transl Med. 2013; 5:193ra191.
6. Raetz M, et al. Parasite-induced TH1 cells and intestinal dysbiosis cooperate in IFN-gamma-dependent elimination of Paneth cells. Nat Immunol. 2013; 14:136–142. DOI: 10.1038/ni.2508 [PubMed: 23263554]
7. Winter SE, Lopez CA, Baumler AJ. The dynamics of gut-associated microbial communities during inflammation. EMBO Rep. 2013; 14:319–327. DOI: 10.1038/embor.2013.27 [PubMed: 23478337]
8. Shin NR, Whon TW, Bae JW. Proteobacteria: microbial signature of dysbiosis in gut microbiota. Trends Biotechnol. 2015; 33:496–503. DOI: 10.1016/j.tibtech.2015.06.011 [PubMed: 26210164]
9. Garrett WS, et al. Communicable ulcerative colitis induced by T-bet deficiency in the innate immune system. Cell. 2007; 131:33–45. DOI: 10.1016/j.cell.2007.08.017 [PubMed: 17923086]
10. Elinav E, et al. NLRP6 inflammasome regulates colonic microbial ecology and risk for colitis. Cell. 2011; 145:745–757. DOI: 10.1016/j.cell.2011.04.022 [PubMed: 21565393]

11. Hughes E, Winter MG, et al. Microbial Respiration and Formate Oxidation as Metabolic Signatures of Inflammation-associated Dysbiosis. Cell Host Microbe. 2017; 21:1–12. [PubMed: 28081439]
12. Winter SE, et al. Host-derived nitrate boosts growth of E. coli in the inflamed gut. Science. 2013; 339:708–711. DOI: 10.1126/science.1232467 [PubMed: 23393266]
13. Gates AJ, et al. Properties of the periplasmic nitrate reductases from Paracoccus pantotrophus and Escherichia coli after growth in tungsten-supplemented media. FEMS Microbiol Lett. 2003; 220:261–269. [PubMed: 12670690]
14. Hans W, Scholmerich J, Gross V, Falk W. The role of the resident intestinal flora in acute and chronic dextran sulfate sodium-induced colitis in mice. Eur J Gastroenterol Hepatol. 2000; 12:267–273. [PubMed: 10750645]
15. Rutgeerts P, et al. Controlled trial of metronidazole treatment for prevention of Crohn's recurrence after ileal resection. Gastroenterology. 1995; 108:1617–1621. [PubMed: 7768364]
16. Prantera C, et al. An antibiotic regimen for the treatment of active Crohn's disease: a randomized, controlled clinical trial of metronidazole plus ciprofloxacin. Am J Gastroenterol. 1996; 91:328–332. [PubMed: 8607501]
17. Stecher B, et al. Salmonella enterica serovar typhimurium exploits inflammation to compete with the intestinal microbiota. PLoS Biol. 2007; 5:2177–2189. DOI: 10.1371/journal.pbio.0050244 [PubMed: 17760501]
18. Collins S, Verdu E, Denou E, Bercik P. The role of pathogenic microbes and commensal bacteria in irritable bowel syndrome. Dig Dis. 2009; 27(Suppl 1):85–89. DOI: 10.1159/000268126 [PubMed: 20203502]
19. Kamada N, et al. Regulated virulence controls the ability of a pathogen to compete with the gut microbiota. Science. 2012; 336:1325–1329. DOI: 10.1126/science.1222195 [PubMed: 22582016]
20. Brugiroux S, et al. Genome-guided design of a defined mouse microbiota that confers colonization resistance against Salmonella enterica serovar Typhimurium. Nat Microbiol. 2016; 2:16215. [PubMed: 27869789]
21. Kruis W, et al. Maintaining remission of ulcerative colitis with the probiotic Escherichia coli Nissle 1917 is as effective as with standard mesalazine. Gut. 2004; 53:1617–1623. DOI: 10.1136/gut.2003.037747 [PubMed: 15479682]
22. Sassone-Corsi M, et al. Microcins mediate competition among Enterobacteriaceae in the inflamed gut. Nature. 2016; 540:280–283. DOI: 10.1038/nature20557 [PubMed: 27798599]
23. Sambrook, J., Maniatis, EFFT. Molecular Cloning. Cold Spring Harbor Laboratory Press; 1989.
24. Davis, RW., D, B., Roth, JR. Advanced Bacterial Genetics. Cold Spring Harbor Laboratory Press; 1980.
25. Price-Carter M, Tingey J, Bobik TA, Roth JR. The alternative electron acceptor tetrathionate supports B12-dependent anaerobic growth of Salmonella enterica serovar typhimurium on ethanolamine or 1,2-propanediol. Journal of bacteriology. 2001; 183:2463–2475. DOI: 10.1128/JB.183.8.2463-2475.2001 [PubMed: 11274105]
26. Caporaso JG, et al. QIIME allows analysis of high-throughput community sequencing data. Nat Methods. 2010; 7:335–336. DOI: 10.1038/nmeth.f.303 [PubMed: 20383131]
27. Shavit Y, Hamey FK, Lio P. FisHiCal: an R package for iterative FISH-based calibration of Hi-C data. Bioinformatics. 2014; 30:3120–3122. DOI: 10.1093/bioinformatics/btu491 [PubMed: 25061071]
28. Li W, Godzik A. Cd-hit: a fast program for clustering and comparing large sets of protein or nucleotide sequences. Bioinformatics. 2006; 22:1658–1659. DOI: 10.1093/bioinformatics/btl158 [PubMed: 16731699]
29. Fu L, Niu B, Zhu Z, Wu S, Li W. CD-HIT: accelerated for clustering the next-generation sequencing data. Bioinformatics. 2012; 28:3150–3152. DOI: 10.1093/bioinformatics/bts565 [PubMed: 23060610]
30. Barman M, et al. Enteric salmonellosis disrupts the microbial ecology of the murine gastrointestinal tract. Infection and immunity. 2008; 76:907–915. DOI: 10.1128/IAI.01432-07 [PubMed: 18160481]

31. Winter SE, et al. Contribution of flagellin pattern recognition to intestinal inflammation during Salmonella enterica serotype typhimurium infection. Infect Immun. 2009; 77:1904–1916. DOI: 10.1128/IAI.01341-08 [PubMed: 19237529]
32. Winter SE, et al. Gut inflammation provides a respiratory electron acceptor for Salmonella. Nature. 2010; 467:426–429. DOI: 10.1038/nature09415 [PubMed: 20864996]
33. Bacchetti De Gregoris T, Aldred N, Clare AS, Burgess JG. Improvement of phylum- and class-specific primers for real-time PCR quantification of bacterial taxa. J Microbiol Methods. 2011; 86:351–356. DOI: 10.1016/j.mimet.2011.06.010 [PubMed: 21704084]
34. Stewart V, Parales J Jr. Identification and expression of genes narL and narX of the nar (nitrate reductase) locus in Escherichia coli K-12. Journal of bacteriology. 1988; 170:1589–1597. [PubMed: 2832370]
35. Rodriguez MS, Thompson J, Hay RT, Dargemont C. Nuclear retention of IkappaBalpha protects it from signal-induced degradation and inhibits nuclear factor kappaB transcriptional activation. The Journal of biological chemistry. 1999; 274:9108–9115. [PubMed: 10085161]
36. Keestra AM, et al. A Salmonella virulence factor activates the NOD1/NOD2 signaling pathway. mBio. 2011; 2
37. Eaves-Pyles T, et al. Escherichia coli isolated from a Crohn's disease patient adheres, invades, and induces inflammatory responses in polarized intestinal epithelial cells. Int J Med Microbiol. 2008; 298:397–409. DOI: 10.1016/j.ijmm.2007.05.011 [PubMed: 17900983]
38. Kim SC, et al. Variable phenotypes of enterocolitis in interleukin 10-deficient mice monoassociated with two different commensal bacteria. Gastroenterology. 2005; 128:891–906. [PubMed: 15825073]
39. Pal D, Venkova-Canova T, Srivastava P, Chattoraj DK. Multipartite regulation of rctB, the replication initiator gene of Vibrio cholerae chromosome II. Journal of bacteriology. 2005; 187:7167–7175. DOI: 10.1128/JB.187.21.7167-7175.2005 [PubMed: 16237000]
40. Simon R, Priefer U, Puhler A. A Broad Host Range Mobilization System for In Vivo Genetic Engineering: Transposon Mutagenesis in Gram Negative Bacteria. Nature Biotechnology. 1983; 1:784–791. doi: DOI: 10.1038/nbt1183-784
41. Overbergh L, et al. The use of real-time reverse transcriptase PCR for the quantification of cytokine gene expression. J Biomol Tech. 2003; 14:33–43. [PubMed: 12901609]
42. Godinez I, et al. T cells help to amplify inflammatory responses induced by Salmonella enterica serotype Typhimurium in the intestinal mucosa. Infect Immun. 2008; 76:2008–2017. DOI: 10.1128/IAI.01691-07 [PubMed: 18347048]
43. Wilson RP, et al. The Vi-capsule prevents Toll-like receptor 4 recognition of Salmonella. Cell Microbiol. 2008; 10:876–890. DOI: 10.1111/j.1462-5822.2007.01090.x [PubMed: 18034866]
44. Wang RF, Kushner SR. Construction of versatile low-copy-number vectors for cloning, sequencing and gene expression in Escherichia coli. Gene. 1991; 100:195–199. [PubMed: 2055470]

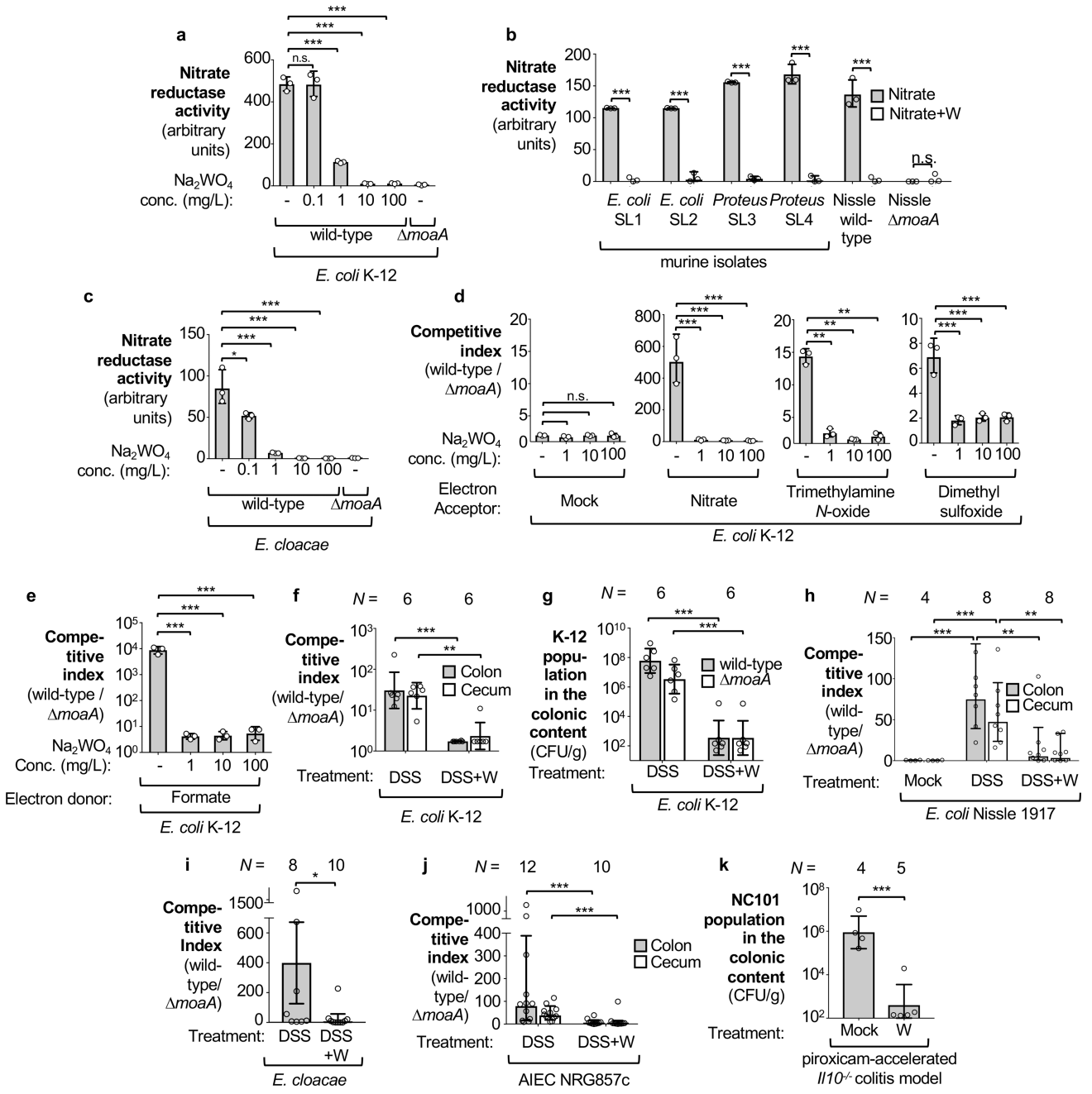


**Figure 1. Effect of tungstate on molybdenum cofactor-dependent anaerobic respiration**

**a–c** Nitrate reductase activity in *E. coli* K-12 (**a**), commensal Enterobacteriaceae strains (**b**) and an *Enterobacter cloacae* strain (**c**). **d–e** Competitive anaerobic growth of the *E. coli* K-12 wild type and a *moaA* mutant in the presence of electron acceptors (**d**) or microaerobic growth with the electron donor formate (**e**). **a–e**, $n$=3 replicates for each condition. **f–j** C57BL/6 mice received tungstate (W), dextran sulfate sodium (DSS), and DSS+W in the drinking water for 4 days. Animals were intragastrically inoculated with an equal mixture of the indicated *E. coli* wild-type strains and isogenic *moaA* mutants. *E. coli* populations in the cecal and colonic content were analyzed 5 days after inoculation: competitive index (**f**) and

total population (**g**) of *E. coli* K-12; competitive index for Nissle 1917 (**h**), *E. cloacae* (**i**) and NRG857c (**j**). **f–g**, $n$=6 per group. **h**, Mock ($n$=4), DSS ($n$=8), DSS+W ($n$=8). **i**, DSS ($n$=8), DSS+W ($n$=10). **j**, DSS ($n$=12), DSS+W ($n$=10). **k,** *Il10*$^{-/-}$ mice on piroxicam-fortified diet were intragastrically inoculated with the murine *E. coli* strain NC101 and received W in the drinking water or were mock-treated. Abundance of NC101 was assessed after 14 days, Mock ($n$=4), W ($n$=5). Unless stated otherwise, $n$ indicates the number of animals per group. Bars represent geometric means ± geometric standard deviation. *, $P < 0.05$; **, $P < 0.01$; ***, $P < 0.001$; ns, not statistically significant.

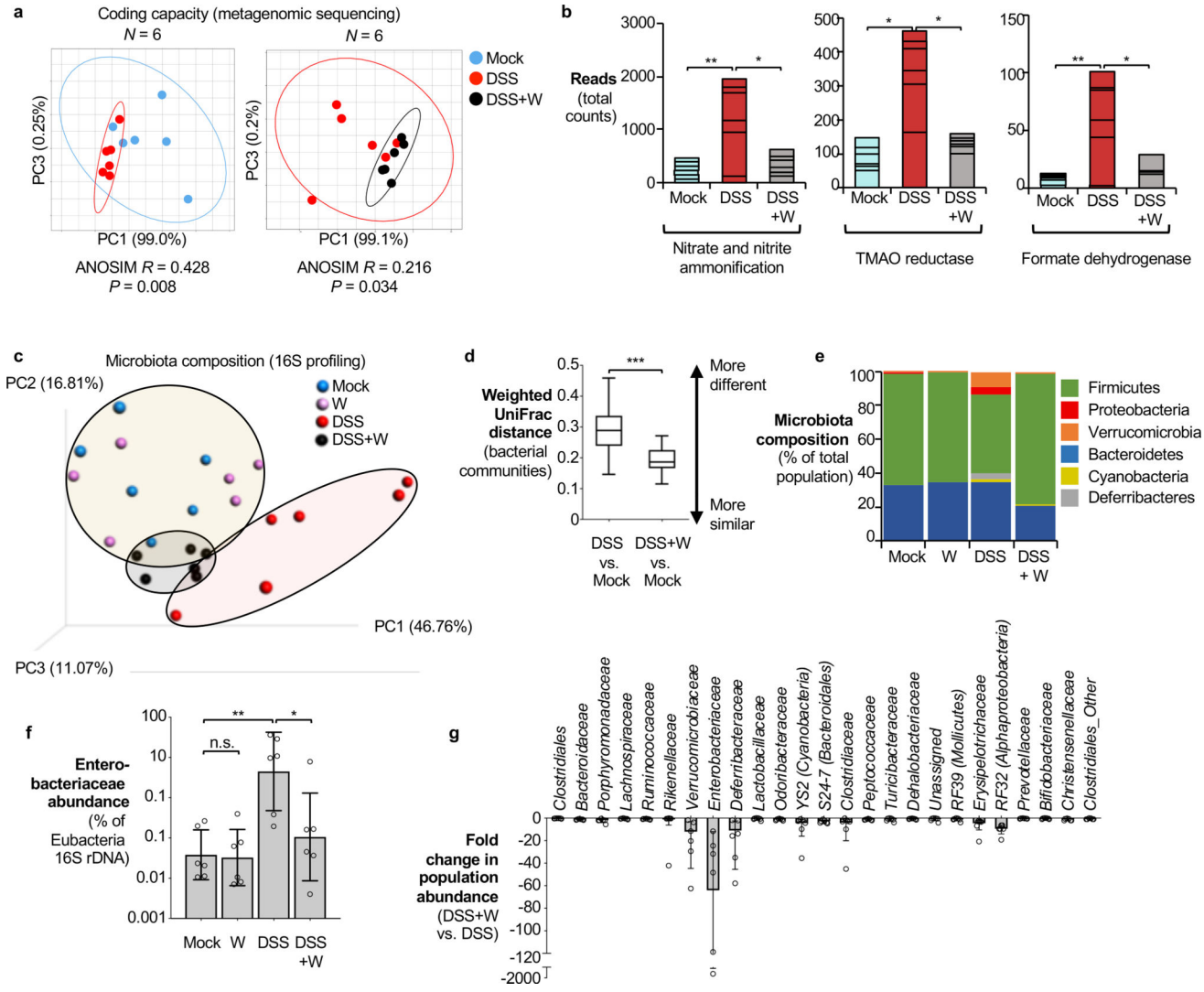


**Figure 2. Impact of tungstate treatment on gut bacterial community composition and metabolic landscape**

DNA extracted from the cecal contents of C57BL/6 mice (*n*=6/group) receiving indicated treatment was analyzed by metagenomic sequencing and 16S profiling. **a,** Principal coordinates (PC) analysis plots and analysis of similarity (ANOSIM) of the predicted coding capacity. Ellipses denote 95% confident interval. The number of animals per group (*N*) is indicated above each graph. **b,** Tallied metagenomic reads mapped to anaerobic respiration and formate utilization pathways. **c,** PC analysis of the microbiota composition (weighted UniFrac distances). **d,** Box-and-whisker plot (Min to Max) of intercommunity β-diversity determined by weighted 16S UniFrac distances. **e,** Phylum-level microbiota composition. **f,** Enterobacteriaceae abundance quantified by qPCR. **g,** Changes in the population size of the 25 most abundant operational taxonomic units as the result of tungstate administration in the DSS colitis model.

Unless noted otherwise, bars represent geometric means ± geometric standard deviation. *, $P < 0.05$; **, $P < 0.01$; ***, $P < 0.001$; ns, not statistically significant.

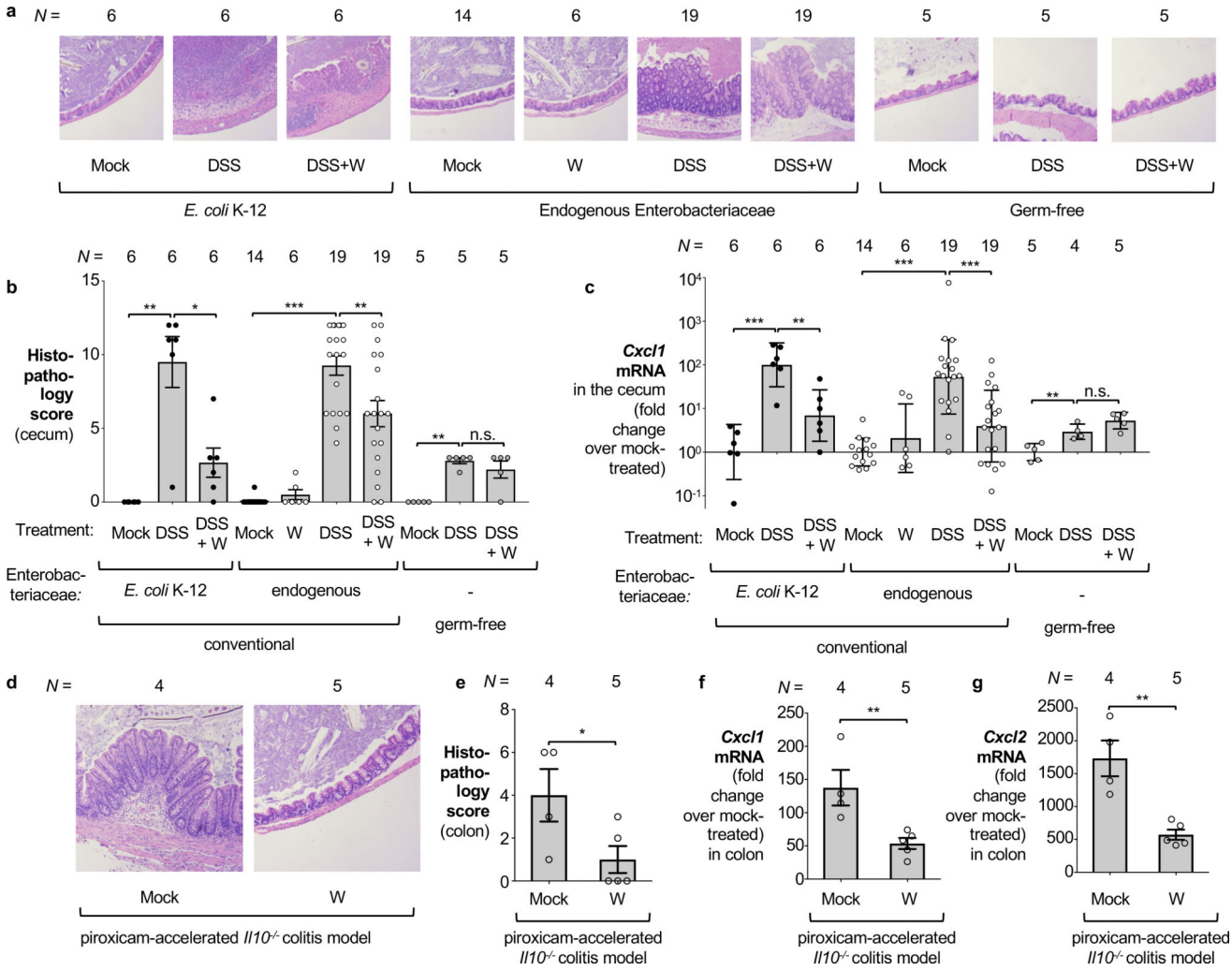


**Figure 3. Influence of tungstate treatment on mucosal inflammation**

**a–c** Conventionally raised C57BL/6 mice, treated with DSS or DSS+tungstate (W) for 4 days, were inoculated with *E. coli* K-12 and samples analyzed after 5 days. C57BL/6 mice with a naïve microbiota (including endogenous Enterobacteriaceae) or germ-free C57BL/6 mice were similarly treated with W, DSS, and DSS+W. *E. coli* K-12: $n$=6 for all groups; Endogenous Enterobacteriaceae: Mock ($n$=14), W ($n$=6), DSS ($n$=19), DSS+W ($n$=19); Germ-free: $n$=5 for all groups (for one DSS-treated mouse, no mRNA was obtained). **a,** Representative images of H+E stained cecal sections. **b,** Cumulative histopathology score for the cecum; Bars represent means ± standard error and each dot represents one animal. **c,** Transcription of *Cxcl1* (*Kc*) in the cecal mucosa by RT-qPCR. **d–g** Groups of *Il10*$^{-/-}$ mice were orally inoculated with NC101. Animals received piroxicam-fortified diet or piroxicam-fortified diet plus tungstate in the drinking water for 2 weeks, Mock ($n$=4), W ($n$=5). **d,** Representative images of H+E stained colonic sections. **e,** Cumulative histopathology score for the colon; Bars represent means ± standard error and each dot represents one animal. Abundance of *Cxcl1* (**f**) and *Cxcl2* (**g**) mRNA in the colonic mucosa by RT-qPCR.

Unless noted otherwise, bars represent geometric means ± geometric standard deviation. *, $P < 0.05$; **, $P < 0.01$; ***, $P < 0.001$; ns, not statistically significant.